Growth of a flat Mn monolayer on Ag(001)

P. Schieffer, C. Krembel, M. C. Hanf, and G. Gewinner

Laboratoire de Physique et de Spectroscopie Electronique, Faculté des Sciences et Techniques, 4 rue des Frères Lumière,
F-68093 Mulhouse Cédex, France

(Received 16 May 1997)

We have carefully investigated the possibility of preparing a well-ordered $p(1\times1)$ two-dimensional Mn monolayer on Ag(001) by means of photoelectron diffraction. It is found that a flat monolayer (ML) with a good degree of perfection is actually achieved by deposition at low rates (typically 0.1–0.2 ML/min) on a substrate held at 80 K. Substrate temperatures higher than ~130 K invariably result in the exchange of Mn adatoms with Ag and the formation of a surface alloy. Valence-band photoemission indicates a giant atomic-like magnetic moment in the flat monolayer, essentially the same as in dilute Ag-based Mn alloys. Most interestingly, low-energy electron diffraction reveals a very sharp $p(1\times1)$ chemical cell pattern with weak but sizable $(\frac{1}{2},\frac{1}{2})$ extra spots visible up to about 100 eV and attributed to in-plane $c(2\times2)$ antiferromagnetic order. [S0163-1829(98)01102-3]

I. INTRODUCTION

Theoretical work for a free unsupported as well as for a Ag(001) or Pd(001) supported Mn monolayer predicts an in-plane $c(2\times2)$ antiferromagnetic arrangement with strongly enhanced magnetic moments close to the free atom $^6S_{5/2}$ ground-state value. More generally, most related theoretical investigations predict enhanced moments in monolayer arrangements that adopt generally antiferromagnetic order for early $3d$ transition metals on late $4d$ or $5d$ transition-metal substrates.[1–6] Very similar trends have been predicted recently for free as well as Ag(001) supported $3d$ metal dimers.[7] The physical origin of enhanced local magnetic moments is clear enough. As the interatomic distance between $3d$ elements increases and coordination number decreases the d electrons become more localized, intraatomic correlation and exchange effects are more and more important, and atomic properties such as a large ground-state magnetic moment are restored. The existence of local magnetic moments may or may not be associated with the presence of specific long-range magnetic order depending on system and temperature. While, this is clear in a Heisenberg model or in the limit of total localization with separated atoms where the local moment is maximum but the Curie or Néel temperature is zero, disordered local moments also exists in itinerant electron systems. This can be shown even in bulk phases and a one-electron itinerant model with a large enough intra-atomic exchange interaction for elements near the center of the $3d$ series such as Fe or Mn in body-centered-cubic (bcc) structures above the Néel or Curie temperatures.[8] On the other hand, $3d$ impurities dissolved in noble metals provide well-known examples of dilute systems with large disordered local moments. A typical system is Mn dissolved in Ag with an effective moment as large as $4.8\mu_B$.[9] In this respect, the calculations predict fairly similar local moments on Mn in dimers[7] and monolayers[2] on Ag(001) or in dilute form[10] in bulk Ag. This suggests that local moment formation provides the largest part of the magnetic stabilization and depends rather weakly on structural details as soon as the direct

Mn-Mn interatomic distance d exceeds some critical value (in the Ag case, $d\geq2.89$ Å). Experimental work based on valence band direct and inverse photoemission supports this point of view in the similar case of Cr/Au(001) (Au-based alloy)[11,12] and Cr/Ag(001) (monolayer).[13–15] Indeed one observes essentially the same Cr $3d$ spin split states in these systems where the actual crystallographic structure (alloy versus monolayer) has been firmly established.[11,16] In contrast, the formation of long-range order and coupling between local moments involve smaller more subtle interactions [for instance of Ruderman-Kittel-Kasuya-Yosida (RKKY) type in alloys] that may strongly depend on distance, coordination number, and specific structure. In this respect, evidence of an antiferromagnetic structure has been obtained for a Cr monolayer on Ag(001).[13,16]

Any attempt at this kind of study has to overcome the difficulties in the production of specific well controlled atomic structures such as flat monolayers of $3d$ transition metals on noble metal substrates. Obviously such hetero-structures are *a priori* highly unstable systems from a thermodynamical point of view since a high surface energy material ($3d$ transition metal) is not expected to wet the surface of a low surface energy substrate (noble metal).[17] Yet, the thermodynamic argument applies to bulklike material under equilibrium conditions whereas, for real systems obtained by vacuum deposition, one usually deals with kinetically hindered metastable ultrathin films. In previous work we have demonstrated the successful preparation of a flat well ordered but metastable Cr monolayer on Ag(001) by deposition on a substrate held at 440 K.[16] It was reported later on that similar growth conditions also result in ordered $p(1\times1)$ layers for other metals of the $3d$ transition series.[15] Yet, our recent work[18–21] shows that this is definitely not the case for the Mn/Ag(001) system. Indeed, Mn deposited on Ag(001) held at room temperature (RT), or above, invariably results in a superficial alloy. The latter is even an unstable system at RT whose structure evolves markedly over a time scale of a few hours.[20] Hence we have carefully explored the possibility to grow a flat Mn monolayer on top of Ag(001) at lower tem-

peratures. We find that this can actually be achieved with a good degree of atomic order upon condensing slowly about one monolayer (ML) on Ag(001) held at 80 K. Valence band photoemission reveals that Mn in such a flat monolayer exhibits an atomiclike moment comparable to dilute Mn in Ag. Most interestingly, up to ~ 100 eV, we clearly observe a weak but extremely sharp $c(2\times 2)$ superstructure by means of low-energy electron diffraction (LEED) that we assign to a magnetic superstructure.

II. EXPERIMENT

The experiments were carried out in an UHV chamber ($\sim 2\times 10^{-10}$ mbar) equipped with four-grid LEED optics, angle resolved ultraviolet (ARUPS) and x-ray photoemission (XPS) and photoelectron diffraction (XPD) techniques. Typical energy resolutions in ARUPS and angular resolutions in both ARUPS and XPD were 150 meV and $+/-3°$, respectively. LEED data were collected with a high sensitivity camera. Mn was deposited onto a clean Ag(001) single-crystal surface, prepared by standard methods, at typical rates of $\sim 0.1-0.2$ ML/min range [1 ML equivalent to the Ag(001) surface atomic density] and typical residual pressures below 4×10^{-10} mbar. The amount of deposited Mn was determined by means of a carefully calibrated computer controlled quartz microbalance and cross checked by XPS. We estimate the absolute uncertainty in these determinations to be ~ 0.1 ML.

III. RESULTS AND DISCUSSION

Figure 1 presents typical Mn $2p_{3/2}$ XPD polar profiles collected along the high symmetry [11] and [10] azimuths of the Ag(001) surface square lattice for ~ 0.9 ML Mn deposits on Ag(001) held at various temperatures in the 80–450 K range. At the kinetic energy 848.8 eV of the Al K_α excited photoelectrons the Mn $2p_{3/2}$ intensity modulations are completely dominated by forward scattering.[22] This means that any intensity enhancement along specific directions of emission directly reveals the presence of atoms scattering the photoelectron wave above the Mn emitter. More generally the anisotropies in intensity give quite straightforward information on the atomic order and epitaxy in the form of a forward projected image of the first coordination shells of the emitter. Now, it is immediately clear from data in Fig. 1 that, except for deposition at 80 K, all profiles exhibit a strong forward scattering peak at $\theta = 45°$ along [11] azimuth. More precisely, we find that the 45° peak becomes well marked as soon as the substrate temperature exceeds ~ 130 K during deposition. This definitely rules out the formation of a flat Mn monolayer on the Ag(001) surface at temperatures above ~ 130 K, and implies a reinterpretation of previous work[15] in terms of the Ag-Mn alloy as opposed to Mn monolayer electronic and magnetic properties. The XPD profiles obtained at temperatures in the 130–300 K range can be readily explained in terms of formation of a two layer thick substitutional Ag-based Mn alloy in line with our previous work based on several surface techniques for RT deposits.[18–21] As can be seen, the XPD profile at 200 K is essentially similar to the one obtained for RT deposition. One observes a typical forward scattering peak at $\theta = 45°$ in [11] azimuth which
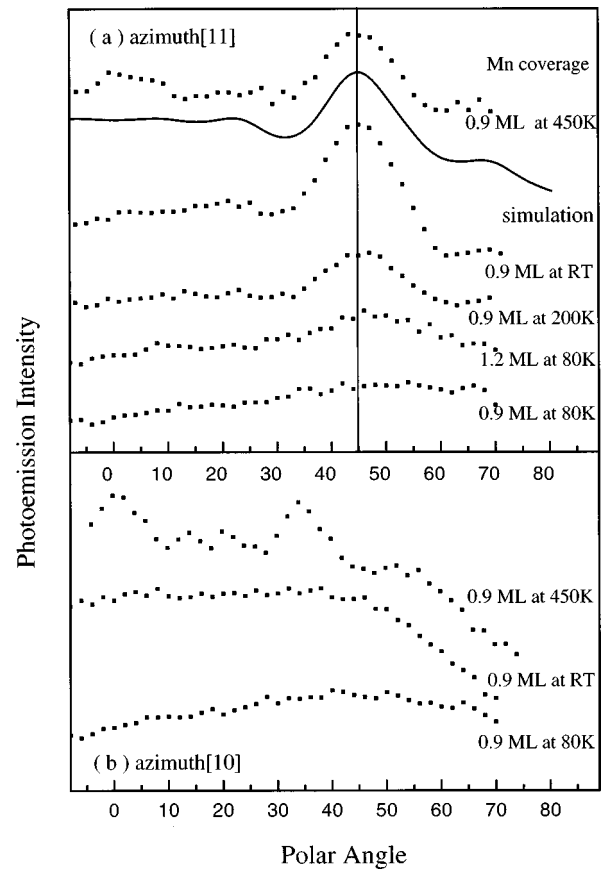
FIG. 1. Angular distribution of the Mn $2p_{3/2}$ core level intensity as a function of coverage and substrate temperatures: along the [11] (a) and [10] (b) azimuths. The line curve represents the calculated Mn $2p_{3/2}$ modulations for a Mn substituting for an Ag atom in the second atomic layer.

corresponds to forward scattering along [101] nearest-neighbor directions of a face-centered-cubic (fcc) lattice. The absence of forward scattering structure along [10] azimuths indicates that the Mn is confined in the two topmost atomic layers of a fcc structure, i.e., the Ag-Mn alloy is only two layer thick. As can be seen the shape and width of the [101] forward scattering peak at 45° along [11] is very well reproduced by single scattering cluster simulations for a Mn substituting for an Ag atom in the second atomic layer. It is interesting to note that, in spite of the large amount ($\sim 50\%$) of Mn substituting for the Ag in the two topmost atomic layers, XPD shows no measurable change in interlayer spacing with respect to pure Ag (2.03 Å). This indicates that the Mn adopts a very large atomic volume for an element of the $3d$ series and suggest a high spin state of the Mn in this alloy as confirmed by ARUPS data shown below.

As discussed in Ref. 20 the surface dynamical process that leads to this superficial Mn-Ag alloy is a thermally activated atomic place exchange mechanism. The present data imply that this mechanism remains active at temperatures down to 130 K. For deposition at 450 K or higher, Fig. 1 shows the appearance of additional (smaller) peaks at $\theta = 0°$ and $\theta = 35°$ along [10] assigned to forward scattering along [001] and [112] rows, respectively. This means that Mn now substitutes for Ag in the third or deeper atomic layers from surface, i.e., a more dilute Ag-based Mn alloy is grown at

higher temperatures. Hence, we conclude that, unless the substrate temperature during deposition is maintained below ~ 130 K, a superficial Mn-Ag alloy is invariably formed. Below ~ 130 K, the Mn monolayer must lie flat on the surface since we observe quite isotropic XPD profiles reflecting the instrument response function. Note that, in the submono-layer range, substitution of Mn atoms in the Ag topmost layer might explain an isotropic XPD profile as well. Yet for a 0.9 ± 0.1 ML Mn deposit the only structure consistent with our data is a single atomic layer of Mn on top of the Ag. At first sight it seems surprising that flat monolayer growth takes place at 80 K since one would expect the Mn to occupy second layer positions before the first layer is completed because of a strongly reduced adatom mobility. Apparently the hot Mn impinging on the surface at 80 K gets initially sufficient mobility to reach monolayer platelet steps and sustain monolayer growth. On the other hand, note that an energy of a few eV becomes available upon formation of Mn-Mn or Mn-Ag bonds at the surface. In this respect let us mention the observation of RHEED oscillations at 80 K for the similar Fe/Ag(100) system, indicating that layer by layer growth may take place at low temperatures.[23] To further test this mode of growth, we have investigated the evolution of the XPD profiles versus Mn coverage for deposition at 80 K. We find that while up to ~ 0.9 ML the Mn $2p_{3/2}$ emission remains quite isotropic, a forward focusing peak progressively develops above this coverage along the [11] azimuth at $\sim 47°$ as can be seen in Fig. 1 for 1.2 ML. We interpret this observation in terms of formation of Mn bilayers in a structure with a reduced interlayer spacing (~ 1.9 Å) as compared to Ag (2.03 Å). This structure is a precursor of the epitaxial body-centered-tetragonal (bct) phase observed at larger coverages.[24,18–20] With increasing thickness of the Mn film the perpendicular spacing decreases from 1.9 Å in bi-layers to 1.66 Å for 3–4 ML and above. In Ref. 24 a small but sizeable modulation was observed in the XPD profile by 0.8 ML indicating some bct Mn bilayer formation at this low coverage. Possibly this small difference with our data stems from the much higher deposition rate (2 ML/min) used in that work which is expected to favor a rougher surface. Hence we conclude that a good realization of the ideal flat Mn monolayer on top of Ag(001) is obtained upon depositing about 0.9 ML Mn at 80 K. In this structure the Mn must be arranged in an ordered $p(1 \times 1)$ two-dimensional (2D) atomic layer occupying the fourfold hollow sites of the underlying Ag(001) plane as actually found in the inverted monolayer configuration formed at higher temperatures.[21]

Figure 2 shows typical angle-resolved ultraviolet photoemission spectra of the Mn $3d$ and Ag $4d$ valence states. The data taken at a polar angle $\Theta = 57.5°$ (referred to the surface normal), along [11] azimuth with a $\hbar\omega = 21.2$ eV probe the $\bar{M}$ point of the Ag(001) surface Brillouin zone. The sharp feature at -3.8 eV initial state energy for clean Ag(001) corresponds to a Tamm surface state of $\bar{M}_3$ symmetry, split off from the top of the Ag $4d$ valence band. Deposition of ~ 0.9 ML Mn completely quenches this feature leaving only a series of strongly damped structures reflecting emission from the Ag bulk electronic structure. The small narrow peak at ~ 3.90 eV is not a remainder of the surface state but originates in emission from a flat X_7 bulk band of
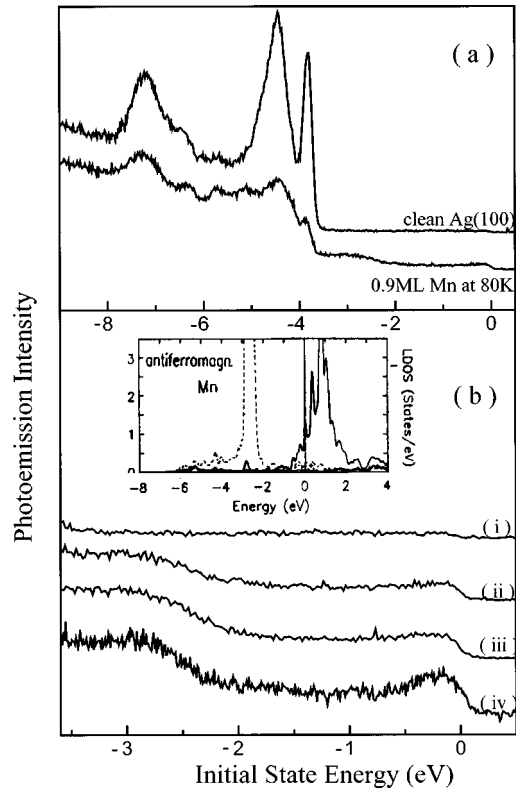
FIG. 2. Typical angle resolved Mn $3d$ and Ag $4d$ valence states photoemission spectra for clean and 0.9 ML Mn deposited at 80 K on Ag(001). (b) Detail of the Mn $3d$-induced states in the 0–4 eV binding energy range: (i) clean Ag(001), (ii) and (iv) 0.9 ML Mn deposited at 80 K (iii) 0.9 ML Mn deposited at RT. The excitation energy is $\hbar\omega = 21.2$ eV and the electrons are collected along [11] azimuth at polar angle $\Theta = 57.5°$ (referred to the sample surface normal) except spectrum (iv) in (b) where $\hbar\omega = 16.8$ eV and $\Theta = 40°$. The inset shows the calculated majority (---) and minority (—) spin densities of states for an ideal Mn monolayer on Ag(001) according to Ref. 1. Negative energies correspond to occupied states, i.e., initial state in photoemission.

Ag along the $\Gamma X K$ symmetry line of the Brillouin zone from which the surface state is split off.[20] Complete quenching of the Tamm surface state and simple attenuation of the bulk Ag features without any shift in binding energy confirm that 0.9 ML Mn deposited on Ag(001) at 80 K forms a sharp interface and lies flat on top of the substrate. Moreover at 80 K and under UHV conditions, this structure is found to be quite stable for hours. This is in sharp contrast with RT deposition which results in an unstable interface that exhibits a shifted Tamm surface state ~ 100 min after deposition.[18,20]

In the 80 K monolayer spectrum emission from Mn $3d$ valence states appears in the form of a fairly broad [~ 0.8 eV full width at half maximum (FWHM)] feature at -2.8 eV as well as a second smaller feature just below the Fermi level. We find no measurable dispersion or splitting of these peaks over the whole two-dimensional Brillouin zone. Neither is there any marked change in the Mn $3d$-induced features upon changing the photon energy. This can be seen in Fig. 2 which compares spectra taken with 21.2 and 16.8 eV photon energies. It means that these photoemission data can be directly compared with the density of states calculated for an antiferromagnetic monolayer on Ag(001) in Ref. 1. As can

be seen there is a very satisfactory agreement between the -2.8 eV feature and calculated majority-spin states on the one hand and the intensity enhancement near Fermi level and the occupied low-energy wing of the minority spin states on the other hand. Yet, Fig. 2 demonstrates that the Mn $3d$-induced features in the alloy formed at higher temperatures closely resemble the ones observed in the 80 K monolayer structure with an occupied majority spin state near -2.8 eV well separated in energy from essentially unoccupied minority spin states. Moreover, quite the same Mn $3d$ feature is observed in valence band photoemission from Mn impurities in Ag (Ref. 25) which are known to bear a local moment of $4\mu_B$ ($S\cong2$).[9] Hence it is apparent that Mn in the 80 K monolayer structure exhibits essentially the same local moment as in Ag-based Mn alloys. Along with inverse photoemission data[15,25] the present finding yields a majority-minority spin Mn $3d$ states splitting in the 4–5 eV range supporting the correlation of about 1 eV/μ_B between splitting and local magnetic moment proposed in Ref. 15. In this respect it is noteworthy that a quite comparable very large $3d$ states splitting has been reported recently for Mn in $c(2\times2)$ surface alloys on Cu(001) and Ni(001).[26] Thus, it appears that photoemission reveals a similar high local magnetic moment on the Mn in all these structures. These data lend further support to the idea put forward in the introduction that beyond a critical Mn-Mn interatomic distance ($d \geq 2.89$ Å) the Mn local magnetic moment shows no strong dependence on specific atomic structure. Yet standard photoemission gives little information on the possible long-range magnetic order which is expected to be quite different in a flat monolayer, intermixed superficial films, or dilute Ag-based alloys.

In this respect, let us now consider the following most interesting LEED observations. For the 80 K flat monolayer structure LEED shows, at all energies E, a very sharp low background pattern which exhibits $p(1\times1)$ periodicity for $E\geq100$ eV, quite comparable to Ag(001). Yet, typical changes in reflected intensities $I(E)$ clearly reveal the presence of a Mn monolayer. This is consistent with a flat monolayer that corresponds to a well ordered $p(1\times1)$ two-dimensional system. Now, below ~100 eV, a weak $c(2\times2)$ superstructure can be clearly seen in the form of additional $(\frac{1}{2},\frac{1}{2})$ spots. Figure 3(a) presents a picture obtained with a high sensitivity charge-coupled device (CCD) camera at normal incidence and $E=40$ eV where the $(\frac{1}{2},\frac{1}{2})$ reflected intensity shows a maximum. Similarly, a fairly strong $(\frac{1}{2},\frac{1}{2})$ beam is found at off normal incidence $i=7.5°$ in the [11] azimuth for $E=22$ eV as can be seen in Fig. 3(b). More generally, at normal incidence we were able to observe the $(\frac{1}{2},\frac{1}{2})$ reflections in the 18–46 eV range with maxima of the integral order beams in the 20–28 eV range and near 32 and 40 eV. Typical relative intensities near maxima in $I(E)$ are $I_{1/2\,1/2}(40\,\text{eV})/I_{10}(40\,\text{eV})\cong6\%$ at normal incidence and $I_{1/2\,1/2}(22\,\text{eV})/I_{00}(36\,\text{eV})\cong3\%$ at $i=7.5°$ in the [11] azimuth. The extrareflections are also visible in the 60–100 eV range but with markedly reduced intensity. This characteristic superstructure is found to be perfectly reproducible, in particular in relative intensity, and visible up to ~130 K where the $p(1\times1)$ Mn monolayer is destroyed by both Mn agglomeration and alloying with Ag.[27] As a function of Mn coverage at 80 K the superstructure can be observed in the

(a)

(b)
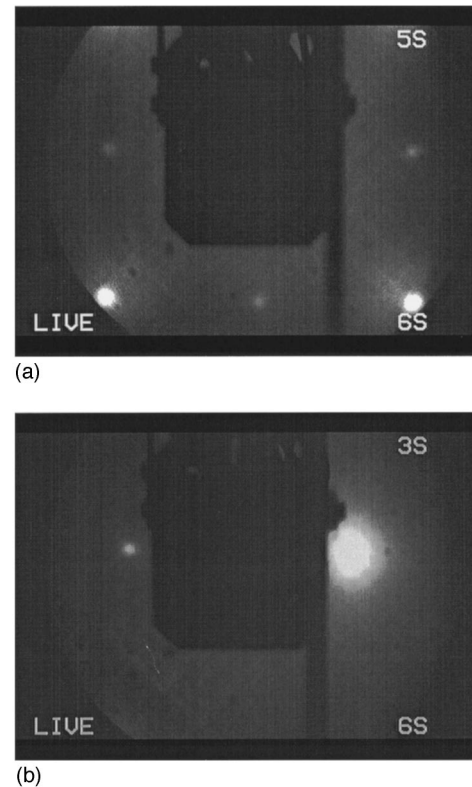
FIG. 3. Typical LEED pictures showing the weak $(\frac{1}{2},\frac{1}{2})$ beam reflections: (a) Normal incidence at $E=40$ eV. (b) Off normal incidence $i=7.5°$ along the [11] azimuth and $E=22$ eV. Note that integral order spots (10) and (01) in (a) and (00) in (b) are strongly overexposed and thus broadened because of the long camera acquisition time ($6s$) needed to make the superstructure visible.

0.6–1.4 ML range with maximum development around 0.9 ML. A remarkable feature concerns the $(\frac{1}{2},\frac{1}{2})$ beam width found to be essentially the same as for integral order beams, as can be seen in the spot profile presented in Fig. 4(a). This indicates the same coherence lengths for $c(2\times2)$ and $p(1\times1)$ long-range order, probably determined by the mean Ag(001) terrace width, and suggests that the $c(2\times2)$ superstructure is an intrinsic feature of the Mn $p(1\times1)$ atomic arrangement. All these specific features are in sharp contrast with those relevant to the $c(2\times2)$ superstructure reported in previous work[19,20,28] for Mn films grown at RT. The latter shows maximum development by 1.5 ML and is readily observed at all energies investigated up to 250 eV with considerably stronger half-order spots. This can be seen in the relevant spot profile scan shown for comparison in Fig. 4(b) which also shows that the coherent $c(2\times2)$ domains are now typically smaller than the $p(1\times1)$ ones. As shown previously[19–20] this kind of $c(2\times2)$ structure reflects the formation of a surface alloy with a mixed Ag-Mn top layer similar to the one formed when Mn is condensed on Cu(001),[29] Pd(001),[30] and Ni(001) (Ref. 31) at RT or above. Finally, we find that this $c(2\times2)$ surface alloy structure exhibits typical $I(E)$ curves in LEED (Ref. 27) quite different from the ones relevant to the weak $c(2\times2)$ superstructure of interest here and observed for a flat monolayer deposited at 80 K. Hence the latter undoubtedly corresponds to a specific superstructure, that cannot be assigned to the $c(2\times2)$ sur-
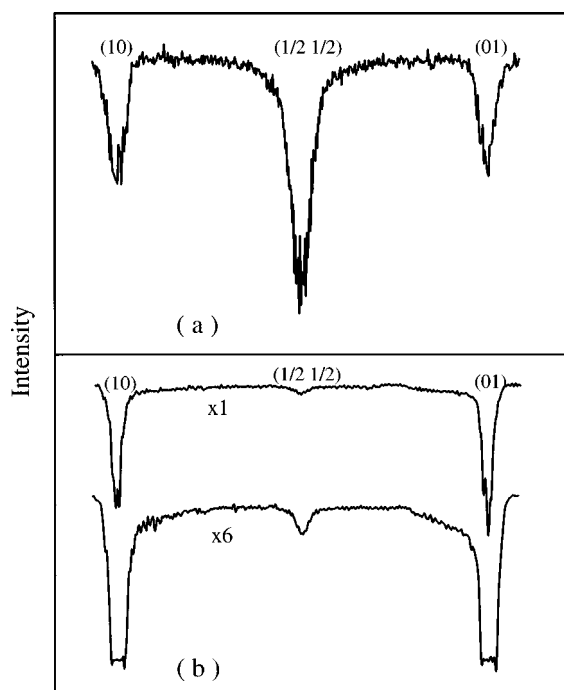
FIG. 4. Spot profile scans through (10) and $(\frac{1}{2}, \frac{1}{2})$ order reflections for (a) the typical $c(2\times2)$ surface alloy formed for Mn deposition at RT. The primary beam energy is $E=66$ eV that corresponds to a maximum in $I(E)$ for the $\frac{1}{2}\frac{1}{2}$ reflection. (b) the faint $c(2\times2)$ superstructure observed for a flat Mn monolayer deposited at 80 K. The primary beam energy is now $E=40$ eV where a maximum in $I(E)$ for the $(\frac{1}{2},\frac{1}{2})$ spot can be seen for this structure. Note the drastic difference in relative spot intensities and widths.

face alloy formed at RT but corresponds to an intrinsic property of the Mn monolayer at 80 K. Actually this superstructure closely resembles the one observed previously on a flat Cr monolayer on Ag(001) and attributed to a magnetic superstructure.[13,16] Theory predicts a $c(2\times2)$ superstructure of magnetic origin with essentially the same local moments for both Cr and Mn monolayers. On the other hand, the phase shifts that describe atomic scattering for Cr and Mn which are neighbors in the periodic table should be essentially the same. Thus the similarity in LEED superstructures observed on ordered $p(1\times1)$ Cr and Mn monolayers on Ag(001) points towards a common physical origin. For Mn as for Cr a magnetic origin is strongly supported by the fact

that the superstructure is essentially detectable below ~ 100 eV only and remains weak at these energies where a sizeable but small difference between scattering amplitudes at spin-up and spin-down Mn atoms due to exchange scattering is expected.[32] In Ref. 32 the ratio of maxima in $I_{1/2\ 1/2}$ and I_{00} was predicted to be about 2% in the 20–60 eV range for a Cr monolayer on Pd(001) at $T=0$ K. Our experimental values for Mn on Ag(001) at 80 K are comparable to this estimation. For Cr on Ag(001) at 300 K, substantially lower extraspot intensities by a factor of about 3 were reported in Ref. 16. This may reflect a difference in overlayer structural quality and/or the lower average local magnetic moment on Cr at 300 K as compared to Mn at 80 K, expected both because of temperature effects and differences in Mn and Cr moments at 0 K. Note that at least within single scattering limit a factor 3 in extraspot intensities means only a factor $\sqrt{3}$ in magnetic moments. Our intensities also compare well with those reported for the first antiferromagnetic structure observed by LEED on NiO surfaces.[33] In contrast, ordinary superstructures based on direct Coulomb scattering such as surface reconstruction, lattice distortions, alloying or chemisorbed impurities are expected to be much stronger [see Fig. 4(b)] and, more importantly, visible in the whole LEED energy range. Moreover, from photoemission data, adsorption of residual gases can be definitely ruled out as a possible origin of the superstructure.

IV. CONCLUSION

To summarize, we have shown that a flat ordered Mn atomic layer can be prepared on Ag(001) by deposition at 80 K at a low rate of ~ 0.2 ML/min. According to photoemission the Mn local magnetic moment in such a layer is about $4\mu_B$, essentially the same as for Mn impurities in Ag. The monolayer shows a typical intrinsic $c(2\times2)$ superstructure that exhibits in every respect the characteristic features expected for exchange scattering from a magnetic structure. Our preliminary investigations indicate that $I(E)$ intensity data of sufficient quality for quantitative exploitation may be obtained for the weak $(\frac{1}{2},\frac{1}{2})$ as well as integral order reflections. Such measurements intended for comparison with dynamical LEED calculations including exchange scattering are presently underway in our laboratory in order to further test and establish (or disprove) the magnetic origin of the $c(2\times2)$ superstructure.

[1] S. Blügel, M. Weinert, and P. H. Dederichs, Phys. Rev. Lett. **60**, 1077 ().

[2] S. Blügel, B. Dritter, R. Zeller, and P. H. Dederichs, Appl. Phys. A: Solids Surf. **49**, 547 (1989).

[3] C. L. Fu and A. J. Freeman, J. Appl. Phys. **61**, 3356 (1987).

[4] G. Allan, Phys. Rev. B **44**, 13 461 (1991).

[5] D. Stoeffler, K. Ounadjela, J. Stich, and F. Gautier, Phys. Rev. B **49**, 299 (1994).

[6] W. Hergert, P. Rennert, C. Demangeat, and H. Dreyssé, Surf. Rev. Lett. **2**, 203 (1995).

[7] V. S. Stepanyuck, W. Hergert, P. Rennert, K. Wildberger, R. Zeller, and P. H. Dederichs, Phys. Rev. B **54**, 14 121 (1996).

[8] V. Heine, J. H. Samson, and C. M. M. Nex, J. Phys. F **11**, 2645 (1981).

[9] C. M. Hurd, J. Phys. Chem. Solids **30**, 539 (1969).

[10] P. J. Braspenning, R. Zeller, A. Lodder, and P. H. Dederichs, Phys. Rev. B **29**, 703 (1984).

[11] M. C. Hanf, C. Pirri, J. C. Peruchetti, D. Bolmont, and G. Gewinner, Phys. Rev. B **36**, 4487 (1987).

[12] M. C. Hanf, C. Pirri, J. C. Peruchetti, D. Bolmont, and G. Gewinner, Phys. Rev. B **39**, 1546 (1989).

[13] C. Krembel, M. C. Hanf, J. C. Peruchetti, D. Bolmont, and G.

Gewinner, Phys. Rev. B **44**, 11 472 (1991).

[14] M. E. Hangan, Q. Chen, M. Onellion, and F. J. Himpsel, Phys. Rev. B **49**, 14 028 (1994).

[15] J. E. Ortega and F. J. Himpsel, Phys. Rev. B **47**, 16 441 (1993).

[16] C. Krembel, M. C. Hanf, J. C. Peruchetti, D. Bolmont, and G. Gewinner, Phys. Rev. B **44**, 8407 (1991).

[17] E. Bauer, Z. Kristallogr. **110**, 372 (1958).

[18] P. Schieffer, C. Krembel, M. C. Hanf, D. Bolmont, and G. Gewinner, Surf. Sci. **352-354**, 823 (1996).

[19] P. Schieffer, C. Krembel, M. C. Hanf, D. Bolmont, and G. Gewinner, Solid State Commun. **97**, 757 (1996).

[20] P. Schieffer, C. Krembel, M. C. Hanf, and G. Gewinner, Phys. Rev. B **55**, 13 884 (1997).

[21] P. Schieffer, M. C. Hanf, C. Krembel, M. H. Tuilier, G. Gewinner, and D. Chandesris, Surf. Rev. Lett. (to be published).

[22] W. F. Egelhoff, Jr., Solid State Mater. Sci. **16**, 213 (1990).

[23] W. F. Egelhoff, Jr. and I. Jacob, Phys. Rev. Lett. **62**, 921 (1989), and references therein.

[24] W. F. Egelhoff, Jr., I. Jacob, J. M. Rudd, J. F. Cohran, and B. Heinrich, J. Vac. Sci. Technol. A **8**, 1582 (1990).

[25] D. Van der Marel, C. Westra, G. A. Sawatzky, and F. U. Hillebrecht, Phys. Rev. B **31**, 1936 (1985).

[26] O. Rader, W. Gudat, C. Carbone, E. Vescovo, S. Blügel, R. Kläsges, W. Eberhardt, M. Wuttig, J. Redinger, and F. J. Himpsel, Phys. Rev. B **55**, 5404 (1997).

[27] P. Schieffer, C. Krembel, M. C. Hanf, and G. Gewinner (unpublished).

[28] D. A. Newstead, C. Norris, C. Binns, A. D. Johnson, and M. G. Barthès, J. Phys. C **21**, 3777 (1988).

[29] M. Wuttig, Y. Gauthier, and S. Blügel, Phys. Rev. Lett. **70**, 3619 (1993).

[30] D. Tian, R. F. Lin, and F. Jona, Solid State Commun. **74**, 1017 (1990).

[31] M. Wuttig, T. Flores, and C. C. Knight, Phys. Rev. B **48**, 12 082 (1993); M. Wuttig and C. C. Knight, *ibid.* **48**, 12 130 (1993).

[32] E. Tamura, S. Blügel, and R. Feder, Solid State Commun. **65**, 1255 (1988).

[33] P. W. Palmberg, R. E. De Wames, and L. A. Vredevoe, Phys. Rev. Lett. **21**, 682 (1988).